Classification of Voltage Sag based on Elliptic Metric

Jiao Hao[1,a], Zongbao Zhang[1,a], Lei Li[2,a], Yonghan Ding[2,a], Liangliang Ge[2,a], Yonggang Wang[2,a] and Lvfu Zhu[3,a,*]

[1]Department of System Operation, Shenzhen Power Supply Bureau Co., Ltd, Guangdong, China

[2]NARI Technology Co., Ltd., Jiangsu, China

[3]Anhui Zeusight Sci. & Tech. Co., Ltd., Hefei, China

[a]zlf715@zeusight.com.cn

*corresponding author

Keywords: Single baseband S transform voltage sag, Ellipse metric, Feature extraction, Classification and recognition.

Abstract: Voltage sag is one of the most serious power quality problems at present. The classification and recognition of voltage sag is the premise and foundation of other voltage research work. In this paper, after adding gauss window with adjustable window width to S transform, four types of voltage sag classification and recognition are realized by using elliptical metric method. The experimental results show that the S transform of single fundamental frequency can accurately judge the amplitude of the sag under different indentation amplitudes. Even if there is relatively large noise interference, its judgment results can meet the requirements. The classification effect of voltage sag based on ellipse metric is better and the recognition rate can reach 99.75%.

1. Foreword

Voltage sag is a very serious power quality problem at present, which is more harmful than harmonic, voltage fluctuation and flicker, three-phase imbalance and other steady state power quality problems. Voltage sag has caused serious harm to power grid, enterprise, factory distribution and power system, and has also caused direct or indirect losses to people's daily life, and more or less affected the overall benefit of national economy. Therefore, to improve and control voltage sag which meet the needs of economic and social development to the greatest extent is the key problem to be solved. In the field of voltage sag research, the classification and recognition of voltage sag is not only the inherent attribute of voltage sag events, but also the premise and foundation of other voltage research work. So, the classification and recognition of depression has a special significance, which must be paid attention to and implemented from now on.

At present, DQ transform[1], Fourier transform[2], short time Fourier transform[3], wavelet transform[4,5] and S transform[6,7] are used in the analysis of voltage sag problem. In Luo's paper[1], the method of dq transform was used to test each eigenvalue, and the real-time compensatory and instantaneous measurement was studied. It was found that its dynamic performance was good, and it was widely used in electric power regulation devices and suitable for real-time and non-real-time situations. Fourier transform is the most widely used method, because it has been put forward for a long time, and there is a relatively large analytical and research ability in the analysis of stable signals, and it has a large proportion in power analysis. But its disadvantage is that it can only analyze some normal stability signals which can satisfy the integrity and orthogonality because of its harsh conditions and poor local transient capability. Based on short time Fourier transform (STFT), the amplitude, duration, source location and classification of voltage sag are studied in reference. A single frequency point and an optimal gauss window width are used in the S-transform calculation. In this paper, the voltage sag analysis method based on the single fundamental frequency S transform is adopted. Four kinds of voltage sag phenomena are studied, and the voltage sag signal is extracted and analyzed. The classification of voltage sag is

  DOI: 10.25236/icbdai.2018.020

realized by Mahalanobis metric.

2. Single Fundamental Frequency S-transform

Single Fundamental Frequency S-transform (SFST) is derived on the basis of S transform. It is the inheritance and development of S transform. Its principle is basically the same as S transform. The difference is that it is only calculated for a single frequency point, and only for the fundamental frequency point is calculated by SFST. The operation time can be greatly reduced. When the voltage sag signal is classified and analyzed, some characteristic quantities of the disturbance signal need to be calculated quickly and accurately, and only the fundamental frequency vector can be calculated to get the desired results. There is no need to calculate the amplitude vectors of all frequency points.

The single fundamental frequency S transform $S(\lambda, f_0)$ of signal $x(t)$ is shown in formula 1.

$$S(\lambda, f_0) = \int_{-\infty}^{\infty} x(t) \frac{|f_0|}{\sqrt{2\pi}} e^{\frac{(t-\lambda)^2 f_0^2}{2}} e^{-j2\pi f_0 t} dt \tag{1}$$

Where f_0 is a fixed frequency, that is the fundamental frequency, and the window function is a Gauss window function, the expression is shown in formula 2.

$$g(\lambda, f_0) = \frac{f_0}{\sqrt{2\pi}} e^{-\frac{\lambda^2 f^2}{2}} \tag{2}$$

The discrete expression of a single fundamental frequency transform is shown in formula 3:

$$S[mT, \frac{n_0}{NT}] = \sum_{m=0}^{N-1} [X(m+n_0) e^{-\frac{2\pi m^2}{n_0^2}}] e^{\frac{2\pi mj}{N}} \tag{3}$$

Where T is the period and n_0 is the sampling point of the fundamental frequency. The one dimensional complex vector is obtained by the upper expression, and the fundamental frequency mode vector is obtained.

S transform is the development of short time Fourier transform and wavelet transform. The width of Gauss window is inversely proportional to frequency and the height is linear to frequency. Different frequencies correspond to different resolutions, which is suitable for analyzing voltage sag.

The expression of S transform S (λ, f) of signal x (t) is shown in formula 4:

$$S(\lambda, f) = \int_{-\infty}^{\infty} x(t) \frac{|f|}{\sqrt{2\pi}} e^{-\frac{(t-\lambda)^2 f^2}{2}} e^{-j2\pi ft} dt \tag{4}$$

The Gauss window function is: $g(\lambda, f) = \frac{|f|}{\sqrt{2\pi}} e^{-\frac{\lambda^2 f^2}{2}}$

In the formula (4) , λ is located in the center of Gauss window, denotes the translation factor, and the position of Gauss window on the time axis is determined, f is frequency, j is imaginary unit.

The signal $x(t)$ can be reconstructed by S transform $S(\lambda, f)$, and the inverse S transform can be obtained as shown in formula 5.

$$x(t) = \int_{-\infty}^{+\infty} \left\{ \int_{-\infty}^{+\infty} S(\tau, f) d\tau \right\} e^{j2\pi ft} df \tag{5}$$

The realization of the discrete form of S transform is based on convolution theorem and Fourier transform. Based on the calculation steps of S transform, the realization steps of single fundamental

frequency S-transform algorithm are as follows:

(1) To judge whether the current input signal is valid or not, then to enter the next step, and the invalid signal needs to be collected again;

(2) The discrete Fourier $X(\mathrm{m})$ is obtained by Fourier analysis of the original signal $x(t)$.

(3) $X(m+n_0)$ was obtained by transposition of $X(\mathrm{m})$.

(4) Taking n_0 as the window center, the Gauss window $G(n_0,m)$ is calculated at the sampling point n_0 of fundamental frequency;

(5) $X(m+n_0)$ is windowed, that is, $X(m+n_0)$ times $G(n_0,m)$, and the sequence $B(n_0,m)$ is obtained.

(6) The inverse Fourier transforms of $B(n_0,m)$ is carried out, and the result of S transform of single fundamental frequency is obtained, which is complex vector $S(j,n_0)$;

(7) S-transform of single fundamental frequency is completed. A fundamental frequency is obtained, which is the modular of $S(j,n_0)$.

The algorithm of single fundamental frequency S transform is similar to that of S transform algorithm. The difference is that the single fundamental frequency S transform uses single frequency point and the optimal window width Gauss window, and only solves the fundamental frequency vector for the fundamental frequency point of the signal spectrum. The computational time is greatly reduced.

3. Ellipse Mahalanobis metric

Mahalanobis distance is going to be done in a very simple way, such as calculating the inverse of the covariance matrix, and now it's going to need further learning [8-10]. The distance learning method is usually based on the Mahalanobis distance, and by learning a projection matrix [11]. The distance of the projected samples is smaller than that of the same category, and the distance between the different classes is larger.

The determination of elliptic metric depends on a symmetric matrix $\boldsymbol{\Omega}$, so determining the elliptic metric is to determine the elliptic metric matrix [9-10]. To a certain extent, the statistical properties of the known data reflect the geometric structure of the sample data, so the initial elliptic metric matrix is calculated from the mean value and covariance matrix of the sample data.

For a given sample matrix $X=\begin{pmatrix} x_{11} & x_{12} & \cdots & x_{1N} \\ x_{21} & x_{22} & \cdots & x_{2N} \\ \vdots & \vdots & \ddots & \vdots \\ x_{n1} & x_{n2} & \cdots & x_{nN} \end{pmatrix}$, $\boldsymbol{x}_i=\begin{pmatrix} x_{1i} \\ x_{2i} \\ \vdots \\ x_{ni} \end{pmatrix}$ represents the i[th] sample $1\le i\le N$. $X_j=(x_{j1},x_{j2},...,x_{jN})$, $1\le j\le n$, And m_j is the mean of X_j, Then the matrix sample X can be represented as $X=(X_1,X_2,...,X_n)^{\mathrm{T}}$, so the covariance between X_i and X_j is $\mathrm{cov}(X_i,X_j)=(X_i-m_i)(X_j-m_j)^{\mathrm{T}}/(N-1)$. Therefore, the covariance matrix of the sample matrix x is as shown in formula 6.

$$\boldsymbol{cov}=\begin{pmatrix} \mathrm{cov}(X_1,X_1) & \mathrm{cov}(X_1,X_2) & \cdots & \mathrm{cov}(X_1,X_n) \\ \mathrm{cov}(X_2,X_1) & \mathrm{cov}(X_2,X_2) & \cdots & \mathrm{cov}(X_2,X_n) \\ \vdots & \vdots & \ddots & \vdots \\ \mathrm{cov}(X_n,X_1) & \mathrm{cov}(X_n,X_2) & \cdots & \mathrm{cov}(X_n,X_n) \end{pmatrix} \tag{6}$$

Let $\boldsymbol{m}=(m_1,m_2,...,m_n)^{\mathrm{T}}$, then the initial elliptic metric matrix is defined as shown in formula 7.

$$\boldsymbol{M}_0 = \begin{pmatrix} \boldsymbol{cov}^{-1} & -\boldsymbol{cov}^{-1}\boldsymbol{m} \\ -\boldsymbol{m}^{\mathrm{T}}\boldsymbol{cov}^{-1} & \boldsymbol{m}^{\mathrm{T}}\boldsymbol{cov}^{-1}\boldsymbol{m} + k^2 \end{pmatrix} \tag{7}$$

Where k > 0, the value of k is generally about 3.5, and T means transpose. M is an invertible positive definite symmetric matrix, and the bilinear form N of M is as shown in formula 8.

$$\sigma(\boldsymbol{x}_i, \boldsymbol{x}_j) = (\boldsymbol{x}_i^{\mathrm{T}}, 1)\boldsymbol{M}_0 \begin{pmatrix} \boldsymbol{x}_j \\ 1 \end{pmatrix} = (\boldsymbol{x}_i - \boldsymbol{m})^{\mathrm{T}}\boldsymbol{cov}^{-1}(\boldsymbol{x}_j - \boldsymbol{m}) + k^2 \qquad (k > 0) \tag{8}$$

$\sigma_{x_i x_j}$ is used to denote $\sigma(\boldsymbol{x}_i, \boldsymbol{x}_j)$, and elliptical metrics such as formula 9.

$$d_M(\boldsymbol{x}_i, \boldsymbol{x}_j) = \frac{k}{2\mathrm{i}} \log \left(\frac{\sigma_{x_i x_j} + \sqrt{\sigma_{x_i x_j}{}^2 - \sigma_{x_i x_i}\sigma_{x_j x_j}}}{\sigma_{x_i x_j} - \sqrt{\sigma_{x_i x_j}{}^2 - \sigma_{x_i x_i}\sigma_{x_j x_j}}} \right) \tag{9}$$

The known Mahalanobis distance between sample x_i and sample x_j can be expressed as shown in formula 10.

$$D_M(\boldsymbol{x}_i, \boldsymbol{x}_j) = \sqrt{(\boldsymbol{x}_i - \boldsymbol{x}_j)^{\mathrm{T}} \boldsymbol{M} (\boldsymbol{x}_i - \boldsymbol{x}_j)} \tag{10}$$

The matrix $\boldsymbol{M} \in \mathbf{R}^{d \times d}$ is the inverse matrix of sample x_i and sample x_j covariance matrix, which can be expressed as $\boldsymbol{M} = \boldsymbol{cov}(\boldsymbol{x}_i, \boldsymbol{x}_j)^{-1}$.

4. Experimental results

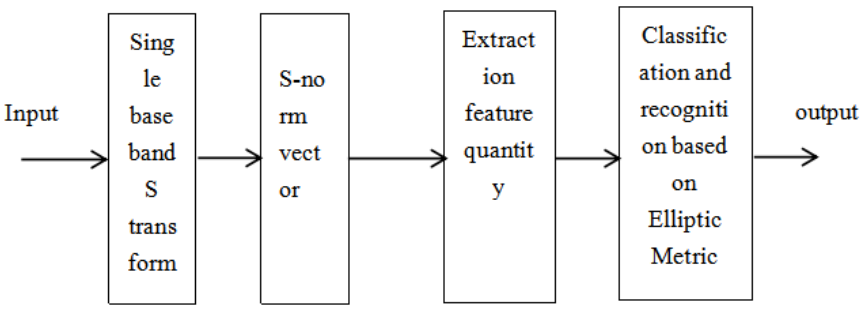

Figure 1 Algorithm flow chart

The block diagram of voltage sag classification algorithm based on ellipse metric is shown in figure 1. The voltage sag and the noise-added voltage sag are simulated and analyzed. The simulation time is 0.4 s and the sampling frequency is 6400 Hz. When 20dB noise is added, the voltage sag waveform is transformed by single fundamental frequency S as shown in Fig. 2.

Fig.2 shows that when the signal to noise ratio of 20dB is added into the voltage sag, the waveform jitter is obvious, which is seriously affected by the noise, which is not conducive to processing and analyzing the signal. However, the difference between the fundamental frequency mode vector and the fundamental frequency mode vector obtained by using the single fundamental frequency S transform is insensitive to noise and can be used to remove noise. The result is not far from the actual situation and can meet the relevant requirements of the system accurately.

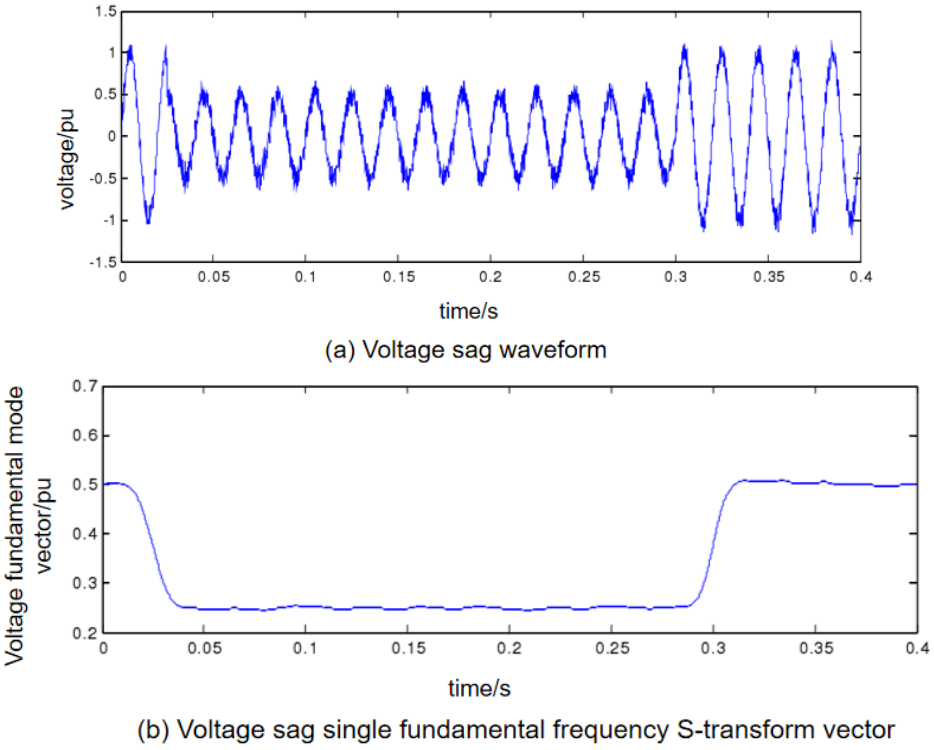

(a) Voltage sag waveform

(b) Voltage sag single fundamental frequency S-transform vector

Figure 2 Analysis of voltage sag waveform under 20dB noise

In this paper, 400 test samples were randomly generated for four voltage sag signals. The sampling time is the same, the sampling frequency is 1.6k Hz, and the signal to noise ratio (SNR) is 20 dB 40dB in each voltage sag test sample. The method proposed in this paper is used to carry out simulation experiments to realize the classification of voltage sag and to verify the accuracy of classification and recognition, as shown in Table 1 and Table 2.

Table 1 Recognition of four types of sag signals with a signal-to-noise ratio of 20dB

Depression type	Number of test samples	Type A	Type B	Type C	Type D	Recognition accuracy %
Type A	400	399	0	0	1	99.75
Type B	400	0	399	1	0	99.75
Type C	400	0	1	399	0	99.75
Type D	400	1	0	0	399	99.75

Table 2 Recognition of four types of sag signals with a signal-to-noise ratio of 40dB

Depression type	Number of test samples	Type A	Type B	Type C	Type D	Recognition accuracy %
Type A	400	400	0	0	0	100
Type B	400	0	400	0	0	100
Type C	400	0	0	400	0	100
Type D	400	0	0	0	400	100

As can be seen in Table 1 and Table 2, the experimental analysis of classification and recognition under noise of 20dB noise shows that the accuracy of recognition under 20dB noise has reached 99.75%。 And under 40dB noise the recognition accuracy can be reach 100%. The higher the signal-to-noise ratio, the higher the accuracy of voltage sag classification. From the simulation results, we can see that the classification method in this paper has high accuracy and strong anti-noise ability.

Because of the same number of amplitude catastrophe points in A and D sag, the number of

amplitude catastrophe points in class B and C sag is the same. It is easy to mix A, D, B and C sags in the critical condition of amplitude. But overall, the correct rate of all kinds of indentation recognition is more than 99.75%. With the increase of signal-to-noise ratio (SNR), the disturbance recognition of voltage sag is almost unaffected, which shows the rationality of the feature extraction method and the voltage sag classifier in this paper.

5. Conclusion

In this paper, the basic principles and algorithms of short time Fourier transform, wavelet transform, S transform and their evolution to single fundamental frequency S transform are described. Four types of voltage sag classification and recognition are realized by ellipse measurement. The principle of S-transform of single fundamental frequency and the elliptic metric are explained emphatically. The experiment's results show that the S transform of single fundamental frequency can accurately judge the amplitude of the sag under different indentation amplitudes. Even if there is a relatively large noise interference, its judgment results can meet the requirements. The classification effect of voltage sag based on ellipse metric is good.

References

[1] Luo Chao, Tao Shun. Rationality analysis of dq transform for transient detection of voltage sag [J]. New Electric Power Technology,2014,33（3）66-70.

[2] Zhang Dong, Wu Xiaoling. Application of short time Fourier transform in Vibration signal processing [J]. Computer and Digital Engineering, 2011, 39(8):154-157.

[3] Xu Yonghai, ZhaoYan. Power quality disturbance Identification based on Short-Time Fourier transform and disturbance time Localization based on sampling singular value decomposition [J]. Grid technology2011, 10(8):174-180.

[4] Qi Bo, Zou Jinhui, YuGangkai. Voltage sag source identification based on Hilbert-Huang transform and wavelet energy spectrum [J]. China electric power, 2013, 08:112-117.

[5] Simon D Kalman filtering with state constrains. A survey of linear and nonlinear algorithms [J]. Control Theory & Applications, IET, 2010, 4(8):1303-1318.

[6] Martin Valtierra-Rodriguez, Rene de Jesus Romero-Troncoso, Roque Alfredo Osornio Rios, et al. Detection and classification of single and combined power quality disturbances using neural networks[J]. IEEE Transactions on Industrial Electronics, 2014, 61(5):2473-2482.

[7] ChenLi, WangShuo, KongWeigong. The characteristic Analysis of compound Voltage drop Source Identification based on improved S transform [J]. Power system protection and control, 2014, 42(4):27-33

[8] NIELSEN F, MUZELLEC B, NOCK R. Classification with mixtures of curved mahalanobis metrics[C]. IEEE International Conference on Image Processing, 2016: 241-245.

[9] Moutafis Panagiotis, Leng Mengjun and Kakadiaris Ioannis. An Overview and Empirical Comparison of Distance Metric Learning Methods[C]. IEEE transactions on cybernetics. 2016, 47(3):1-14.

[10] NIELSEN F, MUZELLEC B, NOCK R. Classification with mixtures of curved mahalanobis metrics[C]. IEEE International Conference on Image Processing, 2016: 241-245.

[11] Ojala. T, Pietikanien. M, and T. Maenpa T. Multiresolution gray-scale and rotation invariant texture classification with local binary patterns[C]. IEEE Trans. on PAMI, 2002, 24(7):971–987.